

# Thickness and Hydraulic Performance of Geosynthetic Clay Liners Overlying a Geonet

S. Dickinson<sup>1</sup>; R. W. I. Brachman<sup>2</sup>; and R. Kerry Rowe, F.ASCE<sup>3</sup>

**Abstract:** Experimental results from physical testing are reported to examine the thickness and hydraulic performance of three geosynthetic clay liners (GCLs) overlying a geonet when subjected to vertical stresses (e.g., as may be found in a secondary leachate collection layer or hydraulic control layer in solid waste landfills). The GCL was found to intrude into the underlying geonet and the effects of GCL type and water content, temperature, applied pressure, and test duration on the final GCL thickness are examined. The results are consistent with GCL deformation from the beneficial consolidation of bentonite as opposed to lateral extrusion of bentonite. Results from fixed ring flow tests suggest that the indentations in the GCL caused by intrusion into the underlying geonet do not appear to negatively impact the hydraulic performance (permittivity or resistance to internal erosion) of the particular GCLs tested for the conditions examined. The flow capacity of the geonet in these tests was found to depend not only on the amount of GCL intrusion but also on the orientation of the geonet relative to the flow direction.

**DOI:** 10.1061/(ASCE)GT.1943-5606.0000247

**CE Database subject headings:** Clay liners; Linings; Landfills; Geosynthetics.

**Author keywords:** Geosynthetic clay liners; Lining, landfills.

## Introduction

Geosynthetic clay liners (GCLs) may be used in conjunction with geomembranes (GMs) and a geonet (GN) as part of a double composite liner separated by a secondary leachate collection system (or leak detection layer) in municipal solid waste landfills as shown in Fig. 1(a). Contaminant transport through the GMs is limited to leakage through small holes in the GM (Rowe et al. 2004; Saidi et al. 2008; Bouazza et al. 2008) and diffusion (especially for nonpolar organic compounds) through the intact GM (Rowe 2005). The primary role of the GCL is to reduce the leakage through any holes that develop in the GM (e.g., see Rowe and Brachman 2004). The GCL may also provide resistance to the diffusive migration of contaminants that pass through the GM (Lake and Rowe 2000a, 2004), although the overall influence on the resistance to diffusive transport may be limited by its small thickness (typically 5–15 mm). The geonet itself provides an opportunity to collect and monitor the fluid collected in the secondary collection system (e.g., Jaisi et al. 2005).

Stresses that develop on these liners from the weight of the

overlying waste could potentially cause the GCL to deform into the geonet as shown in Fig. 1. Shaner and Menoff (1992), Legge and Davies (2002), and Jaisi et al. (2005) all showed that the in-plane flow capacity of a geonet can decrease as a result of GCL intrusion into the geonet. For example, Jaisi et al. (2005) reported flow test results for geonets (thicknesses between 5.0–6.3 mm and masses from 786–1,219 g/m<sup>2</sup>) placed between a GCL (sodium bentonite encapsulated between a woven and a nonwoven geotextile with needle-punching reinforcement) and a GM, and subjected to overburden stress. They reported that for an overburden stress of 200 kPa, the flow rate was reduced to between 53% and 63% of the initial unloaded flow rate depending on the type of geonet used, the type of separating geotextile between the geonet and the GCL, and the hydraulic gradient across the geonet. Each of these studies concluded that, although reduced, adequate flow capacities can be achieved in secondary leachate collection systems using GCLs overlying geonets based on short-term testing. However, there is a paucity of data on the change in GCL thickness and the impact on GCL hydraulic performance when overlying a geonet and subjected to overburden pressures.

As the GCL deforms into the geonet, the GCL would be expected to experience a decrease in thickness as illustrated in Fig. 1(e). If this decrease in thickness is the result of the lateral extrusion of bentonite (e.g., Koerner and Narejo 1995; Fox et al. 2000; Stark et al. 2004; Dickinson and Brachman 2006, 2008), whereby the bentonite experiences shear failure and moves laterally away from the points of contact with the geonet ribs into the adjacent voids in the geonet, then the reduction in GCL thickness could possibly adversely affect the performance of the GCL, since the hydraulic gradient across the GCL at these locations is magnified and hence the leakage would increase since there would be no corresponding decrease in hydraulic conductivity. If the reduction in GCL thickness is the result of the primary consolidation of bentonite, then although the thickness decreases, there would be a corresponding decrease in bulk void ratio of the GCL at the thinner zones. GCL hydraulic conductivity has been

<sup>1</sup>Manager of Engineering, TerrAtlantic Engineering Limited, 515 Beaverbrook Ct., Fredericton NB, Canada E3B 1X6. E-mail: simon@terratlantic.nb.ca

<sup>2</sup>Associate Professor, GeoEngineering Centre at Queen's-RMC, Queen's Univ., Ellis Hall, Kingston ON, Canada K7L 3N6 (corresponding author). E-mail: brachman@civil.queensu.ca

<sup>3</sup>Professor, GeoEngineering Centre at Queen's-RMC, Queen's Univ., Ellis Hall, Kingston ON, Canada K7L 3N6. E-mail: kerry@civil.queensu.ca

Note. This manuscript was submitted on July 21, 2008; approved on September 5, 2009; published online on September 11, 2009. Discussion period open until September 1, 2010; separate discussions must be submitted for individual papers. This paper is part of the *Journal of Geotechnical and Geoenvironmental Engineering*, Vol. 136, No. 4, April 1, 2010. ©ASCE, ISSN 1090-0241/2010/4-552-561/\$25.00.

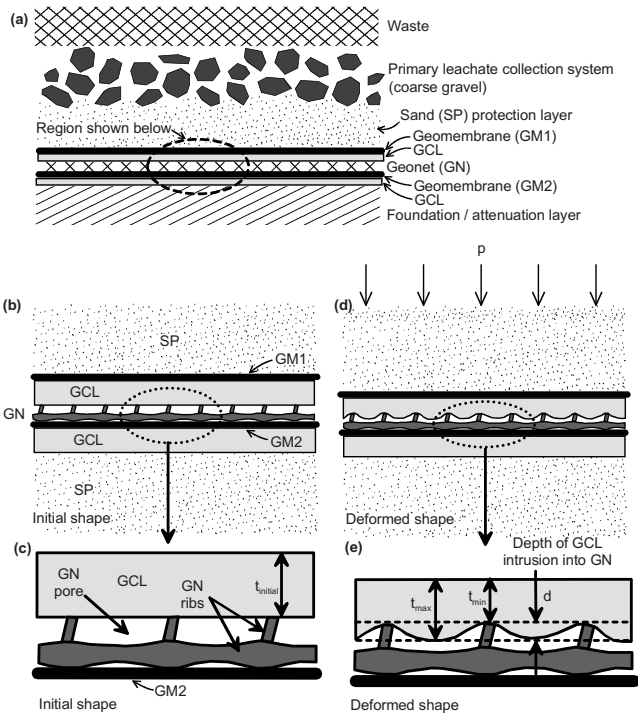


**Fig. 1.** Schematic showing deformation of a GCL overlying a geonet in double liner system

shown to decrease as the bulk void ratio decreases (e.g., Lake and Rowe 2000b; Petrov et al. 1997) and thus the hydraulic performance of the GCL may not be negatively affected.

It is the objective of this paper to assess the impact of one particular geonet on the thickness and hydraulic performance of three different GCL products under various conditions using physical experiments. The effects of overburden pressure, test duration, GCL water content, and temperature on the physical response of the GCL are investigated. Final GCL thickness as well as the depth of GCL intrusion into the geonet is reported. The results from a constant flow rate permeation test on a deformed GCL specimen are presented to examine the hydraulic behavior of the GCL under these conditions. Factors influencing the flow capacity of the geonet are also examined.

## Experimental Details

### GLLS Test Apparatus

A schematic of the geosynthetic liner longevity simulators (GLLSs) used in these experiments is presented in Fig. 2(a). The GLLSs are 0.59-m diameter, 0.5-m tall cylindrical steel pressure vessels capable of applying vertical stresses of up to 1,000 kPa using compressed air on a flexible rubber bladder (Brachman and Gudina 2008a,b). By limiting the outward deflection of the apparatus walls, horizontal stresses corresponding to zero lateral strain were developed. Friction treatment was used to limit the stress reduction in the center of the GLLS from sidewall friction to less than 5%. A temperature control system (involving electrical heating cables, insulation jackets, and controls) was developed for the GLLSs to permit testing at temperatures up to  $85^{\circ}\text{C} \pm 1^{\circ}\text{C}$ .

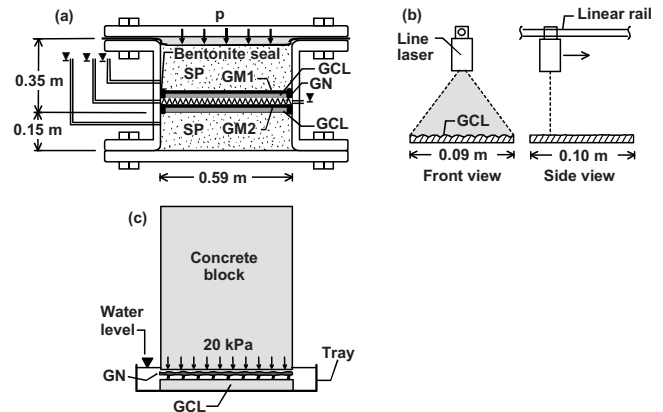


**Fig. 2.** Schematic of (a) test apparatus; (b) line laser; and (c) GCL hydration apparatus

### Configurations and Materials Tested

A total of 24 experiments were conducted in the GLLSs on double composite GM/GCL liners separated by a geonet with the various test configurations summarized in Table 1. Poorly graded medium sand (SP) was used to simulate the case of a stiff foundation layer beneath the GCL. The sand was compacted to a dry density of  $1.9 \text{ g/cm}^3$ . The sand had maximum and minimum dry densities of  $1.95$  and  $1.69 \text{ g/cm}^3$ . In Tests 1–20 the sand was tested at an initial gravimetric water content of approximately  $2 \pm 1\%$ . This water content is representative of the field condition where the groundwater table is well below the foundation layer. In Tests 21–24, the sand was saturated after it was compacted, which is representative of the field condition where the groundwater table is above the foundation layer. The same sand was also used above the primary GM to simulate the case of an excellent protection layer for the GM (e.g., see Dickinson and Brachman 2006, 2008).

Three different GCLs were tested. All consisted of granular sodium bentonite encapsulated between different cover geotextiles and carrier geotextiles, as detailed in Table 2. The mass of bentonite per area for each sample tested was consistent for a given GCL as shown in Table 1. The bentonite in GCL<sub>A</sub> and GCL<sub>B</sub> (which were the same) had a finer gradation than the coarser granular bentonite found in GCL<sub>C</sub>, while both had a similar percentage of montmorillonite and swell index (see Table 2). GCL<sub>A</sub> had a nonwoven cover geotextile and a composite slit-film woven and nonwoven carrier geotextile. GCL<sub>B</sub> had a nonwoven cover and a slit-film nonwoven carrier geotextiles. GCL<sub>C</sub> had two different nonwoven geotextiles. All three GCLs were reinforced by needle-punching and additionally for GCL<sub>A</sub> and GCL<sub>B</sub> the needle-punched fibers were thermally fused to the carrier geotextile. For the purposes of description in this paper, the cover geotextile was defined as the one facing upwards when the GCL was unrolled in its natural orientation, and hence with normal installation the carrier geotextile (bottom) would be in contact with the underlying geonet for a primary composite liner in a double lined landfill. With a bit of effort they may be installed in the field with the cover geotextile facing down for some applications.

The deformations of a GCL overlying a geonet will most certainly be impacted by the water content of the GCL (and hence compressibility and strength of the bentonite) when the vertical pressure is applied, with increasing deformation expected for higher water contents. Given the potential complexities and variabilities in moisture uptake of the GCL in a real application, the

**Table 1.** Test Configurations and Summary of GCL Deformation; Carrier Geotextile Facing Geonet Unless Otherwise Noted

Test	GCL	Applied pressure $p$ (kPa)	Temp. ( $^{\circ}$ C)	Test duration (hrs)	Bentonite mass per area ( $\text{kg}/\text{m}^2$ )	GCL water content $w$ (%)		Final GCL thickness (mm)			GCL intrusion $d$ (mm)
						Initial	Final	Min.	Max.	Mean	
1	GCL <sub>A</sub>	250	22	100	4.0	114	83	4.0	6.6	5.6	1.7
2	GCL <sub>A</sub>	250	35	100	3.8	113	82	4.0	6.6	5.6	1.8
3	GCL <sub>A</sub>	250	55	100	3.9	113	76	3.3	7.0	5.5	2.3
4	GCL <sub>A</sub>	250	55	100	3.8	14	14	4.3	6.8	5.9	1.7
5	GCL <sub>A</sub>	250	55	1,000	4.0	113	60	4.1	7.8	6.4	2.4
6	GCL <sub>A</sub>	750	22	100	3.9	117	64	3.3	7	5.5	2.5
7	GCL <sub>B</sub>	250	22	100	4.5	132	101	5.3	8.7	7.3	2.2
8	GCL <sub>B</sub>	250	35	100	4.6	121	98	4.7	7.8	6.5	2.1
9	GCL <sub>B</sub>	250	55	100	4.6	114	81	3.7	7.4	6.1	2.5
10	GCL <sub>B</sub>	250	55	100	4.5	18	21	3.4	6.4	5.2	1.8
11	GCL <sub>B</sub>	250	22	1,000	4.6	112	84	4.5	7.6	6.4	2.2
12	GCL <sub>B</sub>	250	55	1,000	4.5	115	83	3.1	7.3	5.6	2.8
13	GCL <sub>B</sub>	250	55	2,000	4.5	117	80	3.7	7.6	6.1	2.8
14	GCL <sub>B</sub>	750	22	100	4.6	117	71	3.9	7.9	6.1	2.6
15 <sup>a</sup>	GCL <sub>C</sub>	250	22	100	4.3	176	113	5.2	9.2	7.3	2.7
16 <sup>a</sup>	GCL <sub>C</sub>	250	35	100	4.3	167	108	4.5	13.3	9.4	2.7
17 <sup>a</sup>	GCL <sub>C</sub>	250	55	100	4.5	159	99	6.1	12.2	9.1	2.9
18	GCL <sub>C</sub>	250	55	100	4.4	155	99	4.0	10.2	7.5	3.6
19 <sup>a</sup>	GCL <sub>C</sub>	250	55	1,000	4.3	167	98	5.8	10.3	8.2	3.0
20 <sup>a</sup>	GCL <sub>C</sub>	750	22	100	4.5	175	88	3.7	8.8	6.7	3.0
21 <sup>b</sup>	GCL <sub>A</sub>	250	55	1,000	3.9	123	97	4.3	8.0	6.5	2.4
22 <sup>b,c</sup>	GCL <sub>A</sub>	250	55	1,000	4.0	108	97	5.8	8.9	7.5	1.6
23 <sup>b,c</sup>	GCL <sub>C</sub>	250	55	1,000	4.4	165	124	6.3	10.2	8.6	2.9
24 <sup>b,c</sup>	GCL <sub>A</sub>	250	55	1,000				—			

<sup>a</sup>GCL<sub>C</sub> placed with cover geotextile facing GN.<sup>b</sup>Water introduced to GN throughout test.<sup>c</sup>GT<sub>1</sub> placed between GN and GCL.

approach adopted in this work was to bound the range of initial GCL water contents with a low initial water content as supplied by the manufacturer (Tests 4 and 10 for GCL<sub>A</sub> and GCL<sub>B</sub>, respectively) and much initial higher water contents (for all other tests listed in Table 1) achieved by first immersing the GCL for two weeks in water under a confining stress of 20 kPa [see Fig. 2(c)]. This approach permits the different GCLs to be compared for otherwise identical hydration conditions. The gravimetric water content at the start of each GLLS test is given in Table 1. The impact of the geonet on initial GCL thickness during hydration was also investigated.

Results from index puncture tests following ASTM D4833 (ASTM 2007) performed on the individual cover and carrier geotextiles after being separated from the GCL are given in Table 3. Typical results for the carrier geotextile of GCL<sub>B</sub> are in Fig. 3 along with definition of the offset tensile modulus  $J_{o/s}$ , offset  $\Delta_{o/s}$ , small displacement secant moduli from 0 to 2.5 mm ( $J_{0-2.5\text{ mm}}$ ) and the peak puncture force ( $P_{\text{puncture}}$ ). All carrier and cover geotextiles displaced between 5–10 mm prior to mobilizing appreciable magnitudes of force because of slack in their structure (i.e., as the geotextile deforms the fibers tighten and begin to mobilize its stiffness) as evidenced by the values of offset and

**Table 2.** Details of the GCLs Tested

GCL	Cover geotextile	Carrier geotextile	Detail	Average mass of bentonite ( $\text{kg}/\text{m}^2$ )	Montmorillonite content (%)	CEC <sup>a</sup> (meq/100 g)	Swell <sup>a</sup> index (mL/2 g)	Mean grain size $D_{50}$ (mm)
GCL <sub>A</sub>	Nonwoven needle-punched	Slit-film woven and nonwoven needle-punched	Needle-punched and thermally treated	3.95	50–55	80	23	0.4
GCL <sub>B</sub>	Nonwoven needle-punched	Slit-film woven	Needle-punched and thermally treated	4.55	50–55	80	23	0.4
GCL <sub>C</sub>	Nonwoven needle-punched	Nonwoven needle-punched	Needle-punched	4.39	53–58	120	23	1

Note: CEC=cation exchange capacity.

<sup>a</sup>Reported by Bostwick (2009).

**Table 3.** Description and Index Puncture Test Results of the Geotextiles Tested; the Mean ( $\pm 95\%$  Confidence Intervals) from 15 Specimens of Each Geotextile Tested Are Reported (See Fig. 3 for Definition of Terms)

Type	Mass (g/m <sup>2</sup> )	$J_{o/s}$ (N/mm)	$\Delta_{o/s}$ (mm)	$J_{0-2.5 \text{ mm}}$ (N/mm)	$J_{0-5 \text{ mm}}$ (N/mm)	$P_{\text{puncture}}$ (N)	
<b>GCL<sub>A</sub></b>							
Cover	NW	217	26.2 [ $\pm 2.1$ ]	10.2 [ $\pm 0.5$ ]	0.5 [ $\pm 0.1$ ]	0.9 [ $\pm 0.1$ ]	312 [ $\pm 27$ ]
Carrier	W&NW	242	60.8 [ $\pm 2.5$ ]	7.2 [ $\pm 0.2$ ]	0.8 [ $\pm 0.2$ ]	3.6 [ $\pm 0.5$ ]	426 [ $\pm 14$ ]
<b>GCL<sub>B</sub></b>							
Cover	NW	233	24.7 [ $\pm 1.4$ ]	12.9 [ $\pm 0.4$ ]	0.3 [ $\pm 0.0$ ]	0.4 [ $\pm 0.0$ ]	300 [ $\pm 20$ ]
Carrier	W	123	40.1 [ $\pm 1.2$ ]	5.3 [ $\pm 0.2$ ]	2.4 [ $\pm 0.4$ ]	7.1 [ $\pm 0.7$ ]	274 [ $\pm 12$ ]
<b>GCL<sub>C</sub></b>							
Cover	NW	254	47.1 [ $\pm 4.1$ ]	7.0 [ $\pm 0.5$ ]	2.1 [ $\pm 0.4$ ]	5.42 [ $\pm 0.7$ ]	429 [ $\pm 49$ ]
Carrier	NW	242	21.0 [ $\pm 1.3$ ]	11.3 [ $\pm 0.4$ ]	0.5 [ $\pm 0.0$ ]	0.80 [ $\pm 0.1$ ]	280 [ $\pm 20$ ]
GT <sub>1</sub>	NW	270	47.7 [ $\pm 2.3$ ]	2.9 [ $\pm 0.1$ ]	11.9 [ $\pm 0.6$ ]	22.2 [ $\pm 0.9$ ]	474 [ $\pm 18$ ]

Note: NW=nonwoven, W=woven, and HBNW=heat-bonded nonwoven.

low secant moduli in Table 3. In Tests 1–14, 18, 21–22, and 24, the GCL was placed with the carrier geotextile facing the geonet. In Tests 15–17, 19–20, and 23, GCL<sub>C</sub> was placed with its cover geotextile facing the geonet since the cover geotextile was substantially stiffer than the carrier for GCL<sub>C</sub> and it was hypothesized that this could result in better performance when placed on top of a geonet.

The particular biaxial geonet tested had a thickness of 5.4 mm under a normal stress of 20 kPa. The parallel extruded solid ribs had an open spacing of approximately 9 mm. The average open diagonal span of the geonet was 12 mm. A photograph of the geonet is presented in Fig. 4. No water was added to the geonet during Tests 1–20, while in Tests 21–24, water was introduced to the geonet. High-density polyethylene GMs with thicknesses of 1.5 and 2.0 mm were used in the testing as the primary and secondary GMs, respectively as per Ontario Regulation 232/98 (MoE 1998).

### Quantifying GCL deformation

Following each experiment, the GCL was carefully removed from the GLLS and a line laser was used to measure the final thickness of the central  $0.1 \times 0.09$  m portion of the deformed GCL to an accuracy of 0.04 mm. Fig. 2(b) is a schematic of the line laser apparatus. The laser was mounted on a linear rail and a total of

100 cross sections were taken at 0.001 m intervals. Each cross section was 0.09 m wide and consisted of 1,024 individual points. This technique provides the permanent (i.e., plastic) deformations of the GCL; the amount of elastic rebound of the GCL following stress removal is expected to be small. Although it is the minimum final thickness [ $t_{\text{min}}$  in Fig. 1(e)] which likely controls the hydraulic performance of the GCL, it is difficult to compare tests solely based on this parameter since the final GCL thickness depends on the initial thickness, which varies in each test as a result of the inherent variability in the distribution of bentonite mass in GCLs. As a result an additional metric of GCL deformation was required. Using surface generating software, planes of maximum and minimum GCL thickness [represented as the dashed lines in Fig. 1(e)] were created and the volume between these two planes was calculated. This volume was then divided by the sample area to give the average depth of GCL intrusion into the geonet,  $d$ , as shown in Fig. 1(e).

## Results

### GCL Hydration

Tests H1-H12 were conducted to see the effects of a geonet in contact with one side of a GCL during hydration. In Tests H1-H3,

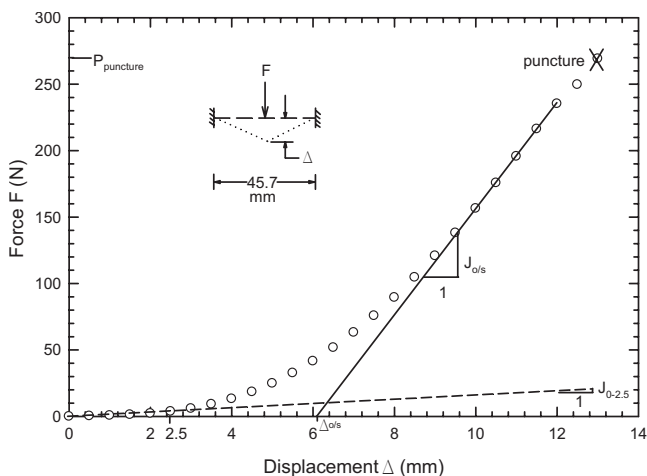


**Fig. 3.** Typical results from index puncture tests [ASTM 4833 (ASTM 2007)] for GCL<sub>B</sub> lower geotextile

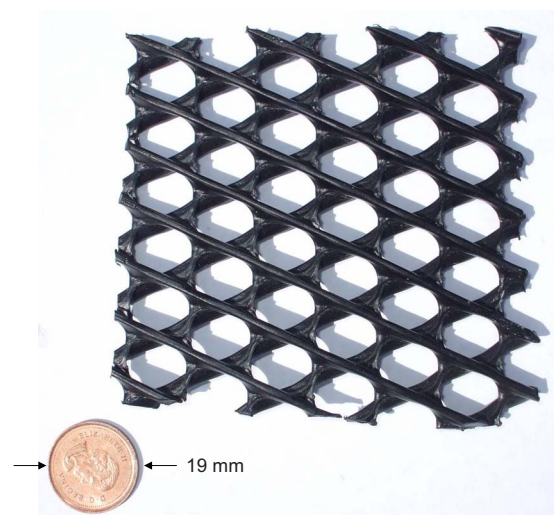


**Fig. 4.** Photograph of geonet

**Table 4.** Results at the End of Two-Week-Long GCL Hydration Tests under 20 kPa Confining Stress; Cover Geotextile of GCL in Contact with a GM; Carrier Geotextile of the GCL in Contact with either a Geonet (GN) or Geotextile (GT)

Test	GCL	Material in contact with GCL carrier GT	Water content of GCL (%)	Thickness of GCL (mm)		
				Min.	Max.	Mean
H1	GCL <sub>A</sub>	GN	113	5.9	8.1	7.1
H2	GCL <sub>A</sub>	GN	115	6.0	7.7	6.8
H3	GCL <sub>A</sub>	GN	112	5.8	7.8	6.9
H4	GCL <sub>A</sub>	GT	110	5.2	7.8	6.7
H5	GCL <sub>B</sub>	GN	127	6.4	9.0	7.6
H6	GCL <sub>B</sub>	GN	113	6.9	9.2	8.1
H7	GCL <sub>B</sub>	GN	110	6.7	8.9	7.8
H8	GCL <sub>B</sub>	GT	111	5.6	8.6	7.3
H9	GCL <sub>C</sub>	GN	131	7.8	12.8	10.1
H10	GCL <sub>C</sub>	GN	174	9.7	13.5	11.6
H11	GCL <sub>C</sub>	GN	143	9.2	12.7	11.1
H12	GCL <sub>C</sub>	GT	142	7.5	11.9	9.7

H5-H7, and H9-H11, a geonet was placed in contact with the carrier geotextile and a GM was placed in contact with the cover geotextile. Water was then introduced into the geonet and the GCL was allowed to hydrate under a confining stress of 20 kPa for a period of two weeks. After this time, the water content and thickness distribution of the GCL were measured. A schematic of the apparatus used in these tests is presented in Fig. 2(c). As a comparison, in Tests H4, H8, and H12, a saturated geotextile was placed in contact with the carrier geotextile of the GCL in place of the geonet and a confining stress of 20 kPa was applied for two weeks.

A summary of results (the minimum, maximum, and mean final GCL thickness for the sample area, as well as the final water content of the GCL) from Tests H1-H12 are presented in Table 4. A contour plot and three-dimensional representation of GCL thickness following hydration from Tests H3 and H4 are presented in Fig. 5. The water contents of the GCLs after two weeks

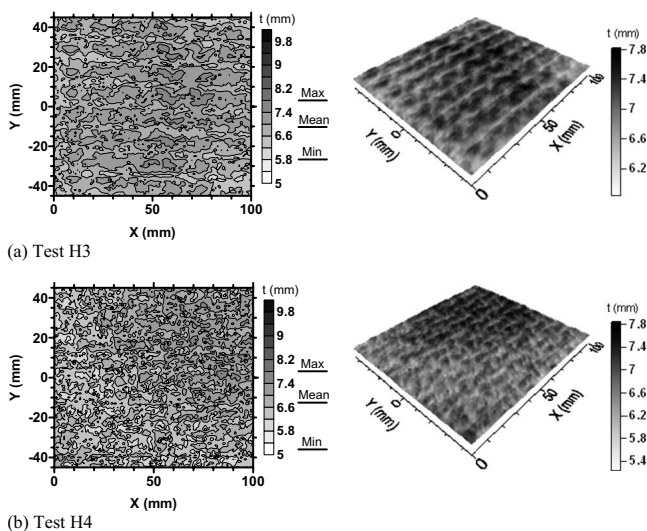


**Fig. 5.** GCL thickness after hydration under 20 kPa for 2 weeks for two cases: (a) geonet in contact with GCL; (b) uniform stress above GCL

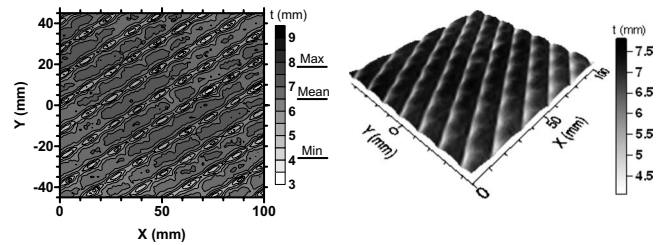


**Fig. 6.** Two-dimensional and three-dimensional representations of GCL thickness following Test 5

are similar for both hydration through a geonet and hydration under a uniform stress. Furthermore, although some indentations appear on the GCL as a result of the geonet ribs [Fig. 5(a)], they are very small, typically with  $d$  less than 1 mm. Hydration under uniform stress conditions resulted in slightly smaller minimum GCL thicknesses than with a geonet but there was no discernable difference in mean and maximum GCL thickness. These results suggest that, overall, for an overburden pressure of 20 kPa, the geonet had very little effect on the GCL during hydration when compared to the same stress applied uniformly. Based on these results, in all other tests where the GCL was prehydrated, the hydration of the GCL was done under a uniform stress block of 20 kPa. Under these conditions the average water content after hydration (with 95% confidence interval) of GCL<sub>A</sub> was 114% ( $\pm 3$ ), 118% ( $\pm 5$ ) for GCL<sub>B</sub> and 166% ( $\pm 6$ ) for GCL<sub>C</sub> (Table 1).

### GCL Deformations

A summary of the initial and final GCL water content, the minimum, maximum, and mean GCL thickness, and the average intrusion of the GCL into the geonet ( $d$ ) for each GLLS test is presented in Table 1.

### Typical Deformed GCL Thickness

A two-dimensional contour plot and three-dimensional surface plot representing final GCL thickness for Test 5 are presented in Fig. 6, where the lighter areas represent thinner regions whereas darker areas represent thicker regions. In all tests, the pattern of GCL deformation was the same. The most apparent indentations were parallel ridges and valleys corresponding to the set of geonet ribs that were in direct contact with the GCL. Along the valleys, a series of regularly spaced concentric thinner regions developed which corresponded to the rib intersections in the geonet. The geonet is thickest at these locations (Fig. 1) and so the GCL deformations at rib intersections are the largest. In some tests (e.g., Tests 6, 14, and 20) the GCL intruded far enough into the geonet that deformations from the second parallel set of geonet ribs became visible. A typical cross section of GCL thickness following Test 5 is presented in Fig. 7. This cross section was taken perpendicular to the orientation of the geonet ribs directly

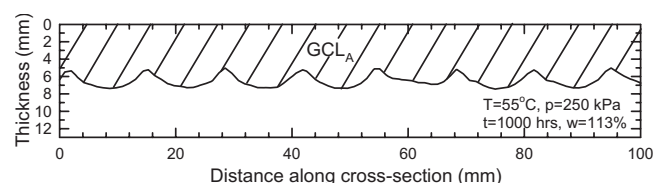


**Fig. 7.** Typical cross section of GCL following Test 5

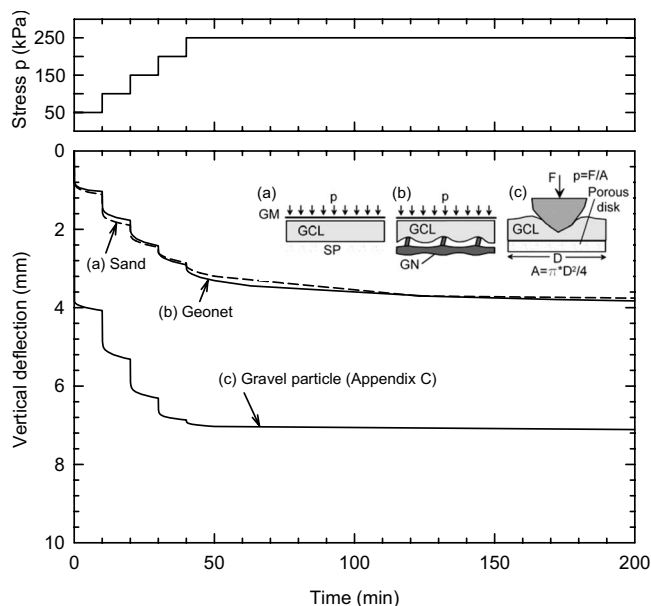


Fig. 8. Results from consolidation test with GCL<sub>B</sub>

in contact with the GCL. The ridges and valleys in the GCL caused by this set of geonet ribs can be seen. In this test, the minimum thickness of the GCL was 4.1 mm and the average GCL intrusion  $d$  was 2.4 mm. Out of all the results in Table 1, the largest GCL deformation occurred in Test 18 for GCL<sub>C</sub>, where the average depth of GCL intrusion was 3.6 mm. The minimum final GCL thickness observed in these tests was 3.1 mm and was recorded in Test 12.

#### Mode of GCL Deformation

In an effort to understand the deformation behavior of a GCL when underlain by a geonet observed in the GLLS tests, two oedometer tests were performed on GCL<sub>B</sub> (Fig. 8). In the first test, a GCL sample with a diameter of 100 mm was prehydrated under a uniform stress of 20 kPa and placed in a fixed wall oedometer over sand (SP) subgrade. A GM was placed above the GCL so that drainage could only occur through the sand. Stress was then applied in increments of 50 kPa every ten minutes up to 250 kPa and deformation was recorded with time. In this test, deformation of the GCL was most certainly from the consolidation of bentonite. This test was then repeated with a geonet beneath the GCL in place of the sand and the results from these two tests are compared in Fig. 8. The rate and magnitude of deformations were nearly identical whether the subgrade was uniform sand or a geonet. This suggests that the observed GCL deformations from the geonet result from bentonite consolidation. To further illustrate this, an example of GCL deformation caused by lateral extrusion of bentonite is also shown in Fig. 8, where the GCL was loaded by an individual gravel particle. In that case, large deformation (four times larger than with uniform loading) of the GCL occurred at low stress levels because the applied stresses exceeded the (very low) available strength of the GCL (Dickinson and Brachman 2004). At higher stresses, consolidation of the bentonite remaining beneath the contact can be seen.

Further evidence that the deformation of the GCL in the GLLS tests was the result of consolidation can be gathered by comparing the GCL thickness results from the GLLS experiments with those from the hydration tests. If deformation was the result of extrusion, there would be very little volume change of the bento-

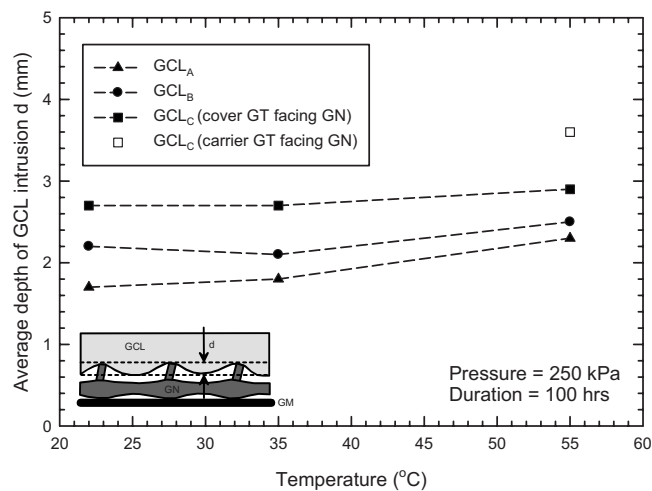


Fig. 9. Effect of temperature on GCL intrusion

nite, and therefore, the areas where the GCL experiences a reduction in thickness would be accompanied by adjacent areas where the thickness has increased (Dickinson and Brachman 2006). The average maximum thickness of GCL<sub>A</sub>, GCL<sub>B</sub>, and GCL<sub>C</sub> in the hydration experiments (with 95% confidence intervals) was 7.9 ( $\pm 0.2$ ), 8.9 ( $\pm 0.2$ ), and 12.7 ( $\pm 0.6$ ) mm, respectively. As shown in Table 1, the maximum thickness of the GCLs in the GLLS experiments was nearly always less. Further, the mean thickness of each GCL in the hydration tests was larger, typically by between 1 and 2 mm, than in the GLLS tests which suggest a net volume reduction of the GCL in the GLLS experiments. Finally, the noticeable decrease in GCL water content (Table 1) from the expulsion of pore water during the test is also indicative of consolidation. Overall, the data strongly suggests that the deformation of the GCL when underlain by a geonet and subjected to load is predominantly the result of primary consolidation of the bentonite. This is very much different to the GCL deformations caused by extrusion of bentonite beneath gravel contacts if the GCL is not adequately protected (Dickinson and Brachman 2006, 2008).

#### Factors Influencing GCL Intrusion into the Geonet

Temperatures at the base of landfills up to 20 to 60°C have been reported depending on the type of waste, age of the landfill, and whether the leachate is being circulated (e.g., Rowe 2005; Koerner and Koerner 2006). To establish the effect of temperature on GCL deformation in a secondary leachate collection system with a geonet, a series of tests were performed for 100 h with an overburden pressure of 250 kPa at temperatures of 22°C, 35°C, and 55°C. A plot of temperature versus GCL deformation, expressed as the average depth of geonet intrusion  $d$ , for each GCL tested is presented in Fig. 9. Temperature has some effect the deformation of the GCL under these testing conditions. For example, for GCL<sub>A</sub>,  $d$  increased from 1.7 to 2.3 mm by increasing the temperature from 22°C to 55°C. It is likely that at elevated temperatures the carrier geotextile of the GCL, which is in contact with the geonet, becomes less stiff, thus allowing the GCL to intrude further into the geonet.

Assuming a unit weight of waste of 13 kN/m<sup>3</sup> and accounting for a frictional loss of 5%, the experiments at an applied pressure of 250 kPa correspond to a thickness of approximately 18 m of waste. To observe the effects of an even higher overburden pressure on GCL deformation for the conditions tested, a series of

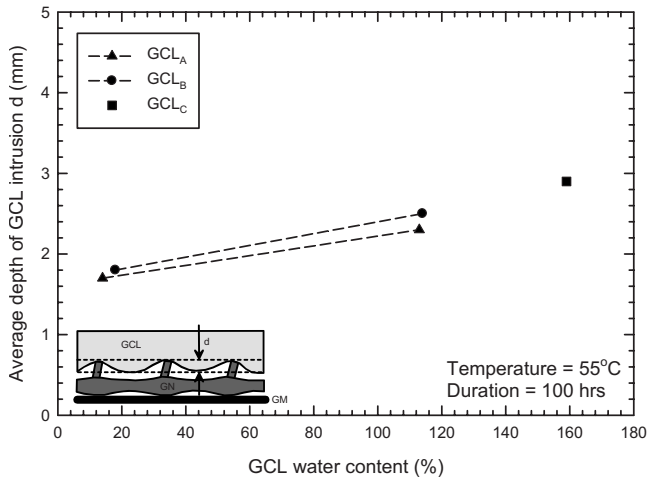


**Fig. 10.** Effect of GCL water content on GCL intrusion

tests were conducted at 750 kPa for 100 h at 22°C. As shown in Table 1, GCL deformation increased with increased overburden pressure. For example for GCL<sub>A</sub>, *d* increased from 1.7 to 2.5 mm as the pressure increased from 250 kPa to 750 kPa (Test 1 versus 6).

Typically, the deformation of the GCL increased slightly with increasing test duration up to 1,000 h (Table 1). For example, for GCL<sub>B</sub>, *d* was calculated to be 2.5 and 2.8 at 100 and 1,000 h, respectively (Test 9 versus 12). No further increase in intrusion was detected for a test on GCL<sub>B</sub> conducted to 2,000 h (*d*=2.8 mm in Test 13).

The higher the initial GCL water content before application of the load, the higher the initial void ratio of the GCL and thus the softer the material. As a result, one would expect that the higher the initial water content, the larger the deformation of the GCL. A plot of the average depth of GCL intrusion for tests performed at 55°C for 100 h with GCLs at different initial water contents is presented in Fig. 10. For example, for GCL<sub>A</sub>, intrusion *d* increased from 1.7 to 2.3 mm by increasing the initial water content from 14% (as supplied) to 113% (hydrated for two weeks under 20 kPa).

The results show that the type of GCL, specifically the extent to which the GCL will swell under a given stress prior to loading as well as the type and stiffness of the geotextile in contact with the geonet, has a distinctive effect on the resulting deformation. This is a function of the geotextiles used and the method of manufacture. GCL<sub>A</sub> and GCL<sub>B</sub> were both thermally treated and this has been shown to decrease the bulk void ratio and thickness of the GCL at hydration relative to GCLs not thermally treated (GCL<sub>C</sub>) due to the fact that the thermal treatment minimizes the pullout of the needle-punched fibers on hydration (Lake and Rowe 2000b). Thus, typically, the deformation of GCL<sub>C</sub> was largest, followed by GCL<sub>B</sub>, and the smallest deformations were observed in GCL<sub>A</sub>. It is likely that the deformations in GCL<sub>A</sub> were smaller than in GCL<sub>B</sub> as a result of the lower initial water content in GCL<sub>A</sub> (Table 1), although the higher offset tensile modulus of the lower (carrier) geotextile in GCL<sub>A</sub> (see Table 3) may have also contributed. The deformations were largest for GCL<sub>C</sub> as compared to the other GCLs primarily as a result of its higher initial water content (under identical hydrating conditions) resulting from the different method of manufacture. The largest deformations were observed in Test 18, where GCL<sub>C</sub> was placed with the lower (carrier) geotextile facing the geonet. As shown in Fig. 9, these deformations

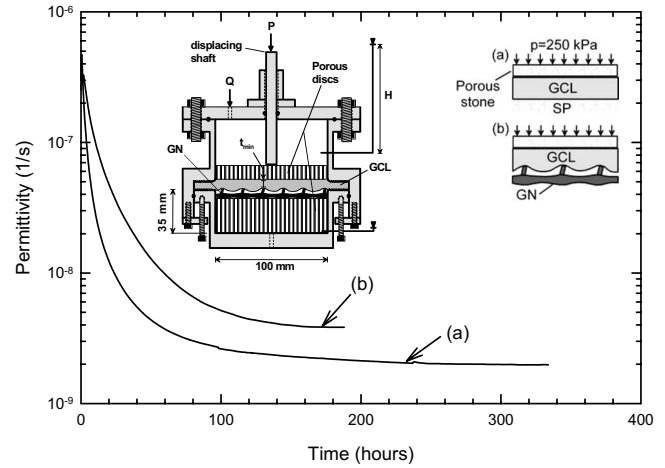


**Fig. 11.** Permittivity of GCL<sub>B</sub> with time

were larger than in the tests where GCL<sub>C</sub> was placed with the upper (cover) geotextile facing the geonet, since the upper geotextile had a much higher stiffness for this particular product (see Table 3).

In a real landfill, fluid may be present in the geonet from small leaks in the primary liner. Once the GCL has deformed, this fluid could potentially cause the GCL to swell into the voids between the geonet ribs, thus further reducing the geonet pore volume. To observe the potential effects of a continuous supply of fluid in the geonet, a number of tests were conducted where the geonet was saturated with water throughout the experiments. The data suggests that the posthydration introduction of water to the geonet had very little effect on the deformation of the GCL. For example, Tests 21 was identical to Test 5 except that in Test 21; water was introduced to the geonet throughout testing. The values of *d* in both of these experiments were calculated to be 2.4 mm. Similarly, in Tests 19 and 23, *d* was calculated to be 3.0 and 2.9 mm, respectively. The lower geotextile appears to resist increases in GCL thickness from swelling between geonet openings.

In Test 22, a 0.6-mm-thick heat-bonded nonwoven geotextile (GT<sub>1</sub>) was placed between the geonet and the GCL. Index properties for this geotextile are given in Table 3. This geotextile was chosen because of its high stiffness at small displacement and low slack (Dickinson and Brachman 2008) relative to other woven and nonwoven geotextiles. The geotextile appeared to have a considerable effect at reducing the deformation of the GCL under the conditions tested. The average depth of geonet intrusion in Test 22 was 1.6 mm—the lowest observed in this study. Further, the minimum GCL thickness recorded in this test was 5.8 mm, which is the largest for any experiment involving GCL<sub>A</sub> conducted.

### Hydraulic Performance of the GCL

To evaluate the hydraulic performance of the deformed GCL, constant flow rate permeation tests were conducted in a 100-mm diameter fixed ring apparatus (Fig. 11). Loose bentonite powder compacted between the GCL and sidewall and a compression seal around the perimeter of the GCL ensured that no leakage of water between the GCL and sidewall occurred.

Two tests were conducted using GCL<sub>B</sub> placed with the woven (carrier) geotextile facing the geonet. In one test the GCL was placed above saturated sand (SP) and a GM was placed above the GCL to serve as a reference case. A uniform pressure of 50 kPa

was applied every 10 min up to 250 kPa, which was maintained for 24 h, allowing full consolidation of the GCL. At this time, the GM was replaced with a porous stone and de-aired tap water was injected into the cell and permeated through the GCL at a constant flow rate of 7.0 mL/hour and the cell pressure was recorded with time [Fig. 11(a)]. The test was conducted at a temperature of 22°C. The second test was nearly the same except that the sand subgrade was replaced with a geonet [Fig. 11(b)]. Permittivity of the GCL with time was calculated from the imposed flow rate and measured cell pressure using Darcy's Law

$$\psi = \frac{Q}{(\Delta H)(A)} \quad (1)$$

where  $Q$ =flow rate;  $\Delta H$ =head difference across the GCL; and  $A$ =cross-sectional area of the apparatus. The advantage of using permittivity in this context—as opposed to hydraulic conductivity—is that although the thickness of the GCL impacts the permittivity, it is not required to calculate the permittivity (hydraulic conductivity is equal to the permittivity multiplied by the thickness).

A plot of permittivity with time for each of these tests is presented in Fig. 11. The steady state permittivity of the GCL when underlain by a geonet was  $3.8 \times 10^{-9} \text{ s}^{-1}$  and when underlain by saturated sand was  $2.0 \times 10^{-9} \text{ s}^{-1}$ . The permittivity was likely higher with a geonet because there is less consolidation in between the geonet ribs [ $t_{\text{max}}$  in Fig. 1(e)]. The increase in permittivity for a GCL overlying a geonet need not be a problem provided that the slightly higher permittivity is taken into account in design. Further, both the GCL tested above sand and geonet had a calculated permittivity below that typically specified by its manufacturer ( $5 \times 10^{-9} \text{ s}^{-1}$  when permeated with de-aired water at an effective stress of 34.5 kPa).

The head difference across the GCL at steady state observed for the tests in Fig. 11 was 125 m and 64 m with sand and geonet subgrades, respectively. The hydraulic gradient created by these large head values are much greater than one would expect to occur in a landfill. These results suggest that for this particular GCL, applied stress, and application in a landfill, where the liner is provided with a suitable protection layer and is therefore loaded uniformly, there may be relatively little risk of failure of the GCL from internal erosion of bentonite since there was no evidence of internal erosion at the very large gradients tested, albeit this test was only conducted for 200 h. Rowe and Orsini (2003) presented results from fixed ring hydraulic conductivity tests, where a GCL with the same cover and carrier geotextiles as  $\text{GCL}_B$  but with a higher mass of bentonite was placed directly over a geonet with a thickness, opening size, and diagonal span of 5.1, 8, and 12 mm, respectively, and a mass of  $790 \text{ g/m}^2$ . A confining stress of 12 kPa was applied prior to two weeks of hydration and remained throughout the tests. They reported that the GCL experienced internal erosion at a head of approximately 19 m. The much higher confining stress (250 kPa versus 12 kPa) and the resulting reduction in void ratio from consolidation is likely the reason why internal erosion did not occur in the fixed ring test presented in Fig. 11. At a confining stress of 250 kPa the contact stresses between the GCL and the geonet ribs are much higher than at 12 kPa. This could be quite significant with the higher stress reducing the mobility of the bentonite particles. It is noted that the geometry of the geonet may also influence the potential for internal erosion and these findings should not be extrapolated to geonets with larger spacings between the ribs than that examined in this study without experimental verification. Based on the find-

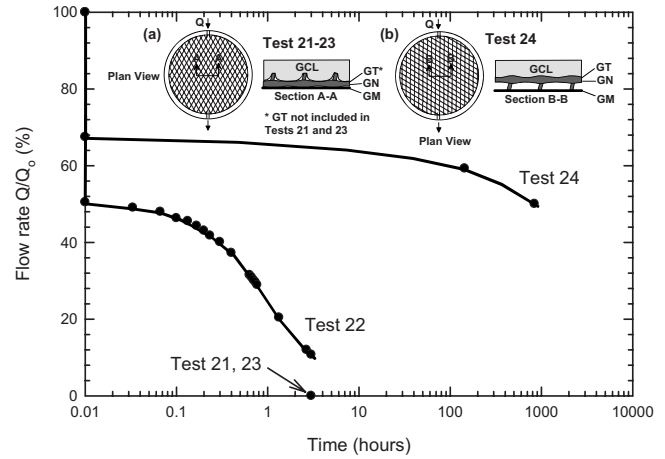


Fig. 12. Flow rate through geonet with time

ings of Rowe and Orsini (2003)  $\text{GCL}_A$  can be expected to perform even better than  $\text{GCL}_B$  with respect to internal erosion. The good performance with respect to internal erosion observed for  $\text{GCL}_B$  and inferred for  $\text{GCL}_A$  may not apply to other GCLs due to the effects of the method of GCL construction; for other GCLs, testing would be required to assess the likelihood of internal erosion when used over a geonet.

### Hydraulic Performance of the Geonet

In Tests 21–24, a constant head reservoir was attached to the GLLS apparatus and the flow rate through the geonet was measured under a gradient of 0.5 [see Fig. 2(a)]. A bentonite seal was placed above and below the geonet to prevent leakage of water into the sand layers. The sand layers above and below the liner were also saturated under the same head as the geonet so as to eliminate any hydraulic gradient between these layers to further ensure that no side leakage would occur. During these flow measurements, the water was introduced at the same temperature as the GLLS. An initial measurement of flow rate was taken before application of the overburden stress so as to provide a baseline for comparison. Subsequent measurements began immediately after the full stress level of 250 kPa had been reached. A plot of flow rate, expressed as a percentage of the flow rate under zero overburden stress, for Tests 21–24 is presented in Fig. 12.

In Tests 21–23, the geonet was oriented as depicted in Fig. 12(a). In Tests 21 and 23 in which the GCL was in direct contact with the geonet, the intrusion of the GCL into the geonet caused the flow rate to stop within 3 h of the stress being applied. This is consistent with the cessation of flow under similar conditions reported by Legge and Davies (2002) and supports their conclusion that a geonet should not be used for a drainage media without a supporting geosynthetic between it and the overlying GCL. In Test 22, with the heat-bonded nonwoven geotextile  $\text{GT}_1$  between the geonet and the GCL, the flow rate immediately after the full overburden stress was reached was 50% of the unloaded flow rate, which then dropped to less than 10% within 3 h of the full stress being reached. In Test 24, the conditions were the same as for Test 22 except that the geonet was oriented as shown in Fig. 12(b). In this test the flow rate immediately after the full overburden stress was reached was 68% of the unloaded flow rate and had still not reached steady state conditions after 1,000 h. It is likely that the geotextile reinforced the GCL over the geonet openings, and over time, the continued decrease in flow capacity

was the result of creep of the geotextile, which led to an increase in GCL intrusion. The decrease in geonet flow capacity is consistent with Jaisi et al. (2005) who reported a flow rate reduction of between 53–63% under a stress of 200 kPa for different geonets and geotextiles. As indicated by the downward trend in flow rate for Test 24 in the first 1000 h (Fig. 12), it is possible that the flow rate in this test would have continued to decrease with time. However, the similarity between the amount of geonet intrusion in Tests 12 and 13 conducted for 1,000 and 2,000 h, respectively, suggests that the majority of geonet intrusion typically occurred in the first 1,000 h; therefore a further reduction in geonet flow capacity after 1,000 h is expected to be small. The difference in flow capacity between Tests 22 and 24 was the result of the geonet orientation. The geonet orientation in Tests 22 and 24 is shown in Fig. 12. In Test 22, the lower set of geonet ribs effectively prevented the flow in the lower half of the geonet as shown in Section A-A of Fig. 12. Flow in the upper half of the geonet was greatly diminished by the deformed GCL and so the flow capacity in the GCL was compromised. In Test 24, even though the pore volume in the upper half of the geonet was reduced as a result of the overlying GCL, the lower half of the geonet remained open and thus the geonet retained some flow capacity. It is unlikely that geonet orientation would have as severe an effect in a landfill as it did in these experiments, where the inflow and outflow were each concentrated through a single port. In a landfill, flow would be expected to occur over a much wider area and therefore the fluid would have an easier time finding its way around an obstruction. However, the results show that even with a geotextile reinforcement layer between the geonet and the GCL, the majority of flow will occur in the lower set of geonet ribs. In critical field applications and laboratory experiments, care should therefore be taken to ensure that the lower set of ribs is oriented in the desired flow direction.

## Discussion

The results suggest that indentations in the GCL caused by intrusion into an underlying geonet do not appear to negatively impact the hydraulic performance (permittivity or resistance to internal erosion) for the particular GCLs and conditions examined. The lower geotextiles of the GCLs do not prevent but do limit GCL intrusion into the geonet once they experience sufficiently large deformations to mobilize their stiffness, and inclusion of a reinforcing geotextile was shown to further reduce the GCL intrusion. However, since the geosynthetic elements of the GCL (geotextiles and needle-punched fibers) appear to be essential to the GCL bridging the openings in the geonet and thereby allow the GCL to perform its intended function as a hydraulic barrier, the long-term performance of a GCL when installed on top of a geonet could be negatively impacted if the service life of the lower geotextile and/or needle-punching fibers of the GCL is reached (e.g., Hsuan and Koerner 2002; Thomas 2002). For example, von Maubeuge and Ehrenberg (2000) suggested conservative service life estimates of 25–50 years for polypropylene fibers. This may be related to the long-term shear strength of GCLs (Müller et al. 2008) since both the application considered here and the long-term shear strength depend on the long-term performance of the fibers.

The tests conducted in this study represent the field case where the GMs are placed with few wrinkles. Wrinkles are known to be present in many landfills (Rowe et al. 2004; Rowe 2005) and a technique has been developed for quantifying wrinkles (Take et al. 2007). A wrinkle in the GM could potentially impact the

physical response of the GCL and geonet by redistributing vertical stresses causing nonuniform loading (e.g., Dickinson and Brachman 2006.)

While the focus of this paper has been on the hydraulic performance of a GCL when placed on top of a geonet, Fitzsimmons and Stark (2002) have postulated that the diffusive flux through the GCL would also likely increase as a result of reduced GCL thickness. Using assumed values of diffusion coefficient, they calculated that the diffusive flux through a GCL with an initial thickness of 7 mm could theoretically increase by a factor of 3 or 4 times should the thickness be reduced to 2 mm as a result of extrusion. The impact of increased diffusion through a GCL deformed by a geonet may warrant assessment; however, if resistance to significant diffusion of, say, volatile organic compounds is required for the double composite liner separated by a geonet shown in Fig. 1, then rather than relying on the thin GCL, one could simply add a soil layer (i.e., the foundation/attenuation layer in Fig. 1) that need not be of exceedingly low hydraulic conductivity (e.g., one of the order of  $10^{-7}$  m/s for say a sandy silt) with its thickness selected to limit diffusion (e.g., see Rowe and Brachman 2004).

## Conclusion

The thickness and hydraulic performance of three different GCL products when overlying a geonet in a secondary leachate collection or leak detection layer and subjected to overburden stresses of 250 kPa and 750 kPa were examined by physical testing. For the particular GCLs and conditions tested, the principal conclusions are

1. GCL thickness: The final GCL thickness was nonuniform having thinner regions that were in direct contact with the geonet ribs and thicker areas that occurred in between the geonet ribs. The amount of GCL intrusion into the geonet increased with increasing GCL water content, temperature, and applied pressure. The lower geotextile of the GCL limited GCL intrusion into the geonet once they experienced sufficiently large deformations to overcome initial slack in their structure and mobilize some stiffness. Inclusion of a reinforcing geotextile between the GCL and geonet did not prevent, but further reduced, GCL intrusion into the geonet. Assessment of the service life of the geosynthetic components of the GCL may be required for the adequate long-term performance of the GCL. The measured results and observations are consistent with GCL deformation from the beneficial consolidation of bentonite and not from lateral extrusion of bentonite;
2. GCL hydraulic performance: The indentations in the GCL caused by intrusion into an underlying geonet did not negatively impact the hydraulic performance (permittivity or resistance to internal erosion) for the practical applications considered over the time frame of the tests. Constant flow permeation testing showed that one particular GCL overlying a geonet and subjected to a uniform stress of 250 kPa had a permittivity of  $3.8 \times 10^{-9} \text{ s}^{-1}$  under a steady state head differential of 64 m relative to a permittivity of  $2.0 \times 10^{-9} \text{ s}^{-1}$  and a steady state head of 125 m when overlying saturated sand. Internal erosion of bentonite did not occur in either test; however this conclusion is only valid for GCL tested and should not be extrapolated to other types of GCL without experimental verification; and
3. Geonet flow capacity: The flow capacity of a geonet can be

greatly reduced from GCL intrusion into the geonet. The presence of a reinforcing geotextile can certainly reduce the GCL intrusion into the geonet and the potential effects from creep, elevated temperatures, and possibly the orientation of the geonet with respect to the flow direction need to be considered. However, in such cases the long-term flow capacity of the geonet will also depend on the service life of the reinforcing geotextile.

## Acknowledgments

This work was funded by the Natural Sciences and Engineering Research Council of Canada through a Strategic Project Grant in partnership with the Ontario Ministry of the Environment, Terrafix Geosynthetics Inc., Solmax International Inc., AECOM, AMEC Earth and Environmental, Golder Associates, CTT Group, and Dr. Grace Hsuan from Drexel University. The experimental infrastructure was developed with funding from the Canada Foundation for Innovation, the Ontario Research Fund, and the Ontario Innovation Trust. Materials were provided by Solmax and Terrafix and BBA Nonwovens. The assistance of Ms. Valerie Latour with the experiments is appreciated.

## References

- ASTM. (2007). "Standard test method for index puncture resistance of geotextiles, geomembranes, and related products (D4833-07)." *Annual book of ASTM standards*, Vol. 04.13, ASTM, West Conshohocken, Pa.
- Bostwick, L. E. (2009). "Laboratory study of geosynthetic clay liner shrinkage when subjected to wet/dry cycles." MS thesis, Queen's Univ., Kingston, Ontario, Canada.
- Bouazza, A., Vangpaisal, T., Abuel-Naga, H., and Kodikara, J. (2008). "Analytical modelling of gas leakage rate through a geosynthetic clay liner-geomembrane composite liner due to a circular defect in the geomembrane." *Geotext. Geomembr.*, 26(2), 122-129.
- Brachman, R. W. I., and Gudina, S. (2008a). "Gravel contacts and geomembrane strains for a GM/CCL composite liner." *Geotext. Geomembr.*, 26(6), 448-459.
- Brachman, R. W. I., and Gudina, S. (2008b). "GM strains and wrinkle deformations in a GM/GCL composite liner." *Geotext. Geomembr.*, 26(6), 488-497.
- Dickinson, S., and Brachman, R. W. I. (2004). "Local deformation of a geosynthetic clay liner from an isolated gravel contact." *Proc., 57th Can. Geotech. Conf.*, Vol. 6D, Québec, 7-11.
- Dickinson, S., and Brachman, R. W. I. (2006). "Deformations of a geosynthetic clay liner beneath a geomembrane wrinkle and coarse gravel." *Geotext. Geomembr.*, 24(5), 285-298.
- Dickinson, S., and Brachman, R. W. I. (2008). "Assessment of alternative protection layers for a geomembrane/geosynthetic clay liner (GM/GCL) composite liner." *Can. Geotech. J.*, 45(11), 1594-1610.
- Fitzsimmons, J. H., and Stark, T. D. (2002). "Theoretical effect of bentonite migration on contaminant transport through GCLs." *Proc., 7th Int. Geosynthetics Conf.*, Taylor & Francis/Balkema, Leiden, The Netherlands, 757-760.
- Fox, P. J., DeBattista, D. J., and Mast, D. G. (2000). "Hydraulic performance of geosynthetic clay liners under gravel cover soils." *Geotext. Geomembr.*, 18(2-4), 179-201.
- Hsuan, Y., and Koerner, R. M. (2002). "Durability and lifetime of polymer fibres with respect to reinforced geosynthetic clay barriers—Reinforced GCLs." *Geosynthetic clay barriers*, H. Zanginger, R. M. Koerner, and E. Gartung, eds., Balkema, 73-86.
- Jaisi, D. P., Glawe, U., and Bergado, D. T. (2005). "Hydraulic behaviour of geosynthetic and granular landfill drainage materials in the Sa Kao landfill, Thailand." *Geotext. Geomembr.*, 23(3), 185-204.
- Koerner, G. R., and Koerner, R. M. (2006). "Long term temperature monitoring of geomembranes at dry and wet landfills." *Geotext. Geomembr.*, 24(1), 72-77.
- Koerner, R. M., and Narejo, D. (1995). "Bearing capacity of hydrated geosynthetic clay liners." *J. Geotech. Geoenviron. Eng.*, 121(1), 82-85.
- Lake, C. B., and Rowe, R. K. (2000a). "Diffusion of sodium and chloride through geosynthetic clay liners." *Geotext. Geomembr.*, 18(2-4), 102-132.
- Lake, C. B., and Rowe, R. K. (2000b). "Swelling characteristics of needle-punched, thermally treated geosynthetic clay liners." *Geotext. Geomembr.*, 18(2-4), 77-101.
- Lake, C. B., and Rowe, R. K. (2004). "Volatile organic compound (VOC) diffusion and sorption coefficients for a needle-punched GCL." *Geosynthet. Int.*, 11(4), 257-272.
- Legge, K. R., and Davies, P. L. (2002). "An appraisal of the performance of geosynthetic materials used in waste disposal facilities in South Africa." *Proc., Waste Conf. (CD-ROM)*, Vol. 2, Durban, South Africa, 321-330.
- MoE. (1998). "Landfill standards: A guideline on the regulatory and approval requirements for the new or expanding landfilling sites." *Ontario Ministry of the Environment, Ontario Regulation No. 232/98*, Toronto, Ontario.
- Müller, W., Jakob, I., Seeger, S., and Tatzky-Gerth, R. (2008). "Long-term shear strength of geosynthetic clay liners." *Geotext. Geomembr.*, 26(2), 130-144.
- Petrov, R. J., Rowe, R. K., and Quigley, R. M. (1997). "Selected factors influencing GCL hydraulic conductivity." *J. Geotech. Geoenviron. Eng.*, 123(8), 683-695.
- Rowe, R. K. (2005). "Long-term performance of contaminant barrier systems." *Geotechnique*, 55(9), 631-678.
- Rowe, R. K., and Brachman, R. W. I. (2004). "Assessment of equivalence of composite liners." *Geosynthet. Int.*, 11(4), 273-286.
- Rowe, R. K., and Orsini, C. (2003). "Effect of GCL and subgrade type on internal erosion in GCLs." *Geotext. Geomembr.*, 21(1), 1-24.
- Rowe, R. K., Quigley, R. M., Brachman, R. W. I., and Booker, J. R. (2004). *Barrier systems for waste disposal facilities*, 2nd Ed., E & FN Spon, London.
- Saidi, F., Touze-Foltz, N., and Goblet, P. (2008). "Numerical modelling of advective flow through composite liners in case of two interacting adjacent square defects in the geomembrane." *Geotext. Geomembr.*, 26(2), 196-204.
- Shaner, K. R., and Menoff, S. D. (1992). "Impacts of bentonite geocomposites on geonet drainage." *Geotext. Geomembr.*, 11(4-6), 503-512.
- Stark, T. D., Choi, H., and Akhtarshad, R. (2004). "Occurrence and effect of bentonite migration in geosynthetic clay liners." *Geosynthet. Int.*, 11(4), 296-310.
- Take, W. A., Chappel, M. J., Brachman, R. W. I., and Rowe, R. K. (2007). "Quantifying geomembrane wrinkles using aerial photography and digital image processing." *Geosynthet. Int.*, 14(4), 219-227.
- Thomas, R. W. (2002). "Thermal oxidation of a polypropylene geotextile used in a geosynthetic clay liner." *Geosynthetic clay barriers*, H. Zanginger, R. M. Koerner, and E. Gartung, eds., Balkema, 87-96.
- von Maubeuge, K. P., and Ehrenberg, H. (2000). "Long-term resistance to oxidation of PP and PE geotextiles." *Proc., 2nd European Geosynthetics Conf.*, Patron Editore, Bologna, Italy, 465-471.